Volume 16, Number 4, 2023. pp. 395-402

Jordan Journal of Physics

ARTICLE

Simulation and Analysis of Field-dependent Measurements for Different a-Si:H and nc-Si:H Samples

R. I. Badran[a,b], **Saja Elnajjar**[b] and **Ahmad Umar**[c,d]

[a] *Physics Department, The Hashemite University, P. O. Box 330127, Zarqa 13133, Jordan.*
[b] *Faculty of Arts and Sciences, Amman Arab University, Amman 11953 P. O. Box 2234, Jordan.*
[c] *Department of Chemistry, Faculty of Science and Arts, Najran University, P. O. Box 1988, Najran-11001, Kingdom of Saudi Arabia.*
[d] *Promising Centre for Sensors and Electronic Devices (PCSED), Najran University, P. O. Box 1988, Najran-11001, Kingdom of Saudi Arabia.*

Doi: https://doi.org/10.47011/16.4.2

Received on: 12/11/2022; Accepted on: 10/01/2023

Abstract: A simulation based on the method of weighted residuals is conducted to reproduce the available experimental data of field-dependent steady-state photocarrier grating (SSPG). Different samples of amorphous hydrogenated silicon (*a*- Si: H) and nanocrystalline hydrogenated silicon (*nc*- Si: H) thin films prepared by plasma-enhanced chemical vapor deposition (PECVD) technique are employed in the simulation. The reproduced field-dependent data are optimized using χ^2 indicator. Approximate and correct values of important photoelectronic parameters are extracted from the analysis of results. The analysis reveals values of small-signal response lifetime and electron and hole mobilities comparable to the values obtained from other methods' applications. The difference between approximate and correct values lies within the experimental error of 5% with one exception regarding a poorly conductive sample. Moreover, the extracted values of both ambipolar diffusion length and charge carrier density are found reasonable and justify the success of the application of the adopted method on the chosen samples.

Keywords: Electronic transport phenomena in thin films; Charge carriers: generation, recombination, lifetime, trapping, mean free paths; Photoconduction and photovoltaic effects.

1. Introduction

The ambipolar diffusion length, L, for minority carriers of amorphous hydrogenated silicon (a-Si: H) material is determined by using the competitive technique of steady-state photocarrier grating (SSPG). Ambipolar diffusion length for various kinds of semiconductors can also be determined using the same technique [1-17]. In the SSPG technique, the sample is illuminated with two beams of light. The first beam exhibits a uniform intensity and creates a uniformly generated background of concentration of carriers. The second beam has a chopped intensity much lower than the first intensity and creates small inhomogeneous concentration of carriers. When the two beams interfere gratings are created on the top of the uniform intensity, with small modulation depth. These gratings are considered as a perturbation of the uniform intensity which consequently yields a small inhomogeneous concentration of carriers (called photocarrier grating (PG)) on the top of uniform concentration of carriers. Thus, two types of photocurrents can be measured: one due to coherent condition and the other due to

Corresponding Author: R. I. Badran **Email**: rbadran@hu.edu.jo ; r.badran@aau.edu.jo

incoherent condition of the two beams [1-3], [10-17]. It is important to indicate here, that to allow for the occurrence of interference, the polarization of light of both beams must be parallel to the electrodes of the sample under study, with electrodes fixed in coplanar geometry. The PG for amorphous or nanocrystalline (nc) semiconductors can only be detected when the width of the grating period, Λ, is very much larger than the carrier diffusion length. Here, the grating period, (defined as $\Lambda = \frac{\lambda}{[2\sin(\frac{\theta}{2})]}$ where λ is the light wavelength), can be adjusted via the angle θ between the two beams [1]. Moreover, the ratio of the two photocurrents (i.e. coherent current/incoherent current), called β, depends on both the size of the grating, Λ, and the electric field, E_o.

Different theoretical approaches were used to solve the problem of a small steady-state photocarrier grating in low and high electric fields [1-8]. Here, various linearization and approximation processes were adopted to solve analytically the nonlinear differential equation (NLDE) for the photoelectrons and photoholes [1-9]. In our approach, the solution of NLDE which represents the amplitude of sinusoidal grating of one cycle interval is taken as approximate one [5]. However, when the nonlinear term is so tiny, this latter solution may be considered correct in our adopted approximation and linearization process. Furthermore, a better solution can be obtained when the method of weighted residuals is employed. This can be achieved if the last solution is initially taken as approximate and the adopted method provides corrections in order to obtain a better solution [5]. Obviously, this will enable us to get a newly corrected expression of β. This corrected expression of β, which is derived as a function of both the grating period and external electric field, can be employed to reproduce field-dependent experimental data of β from the SSPG technique for any noncrystalline semiconductor sample [5]. Furthermore, both approximate and corrected expressions of β comprise important physical quantities. These physical quantities can be employed as free parameters which may give approximate values when the approximate version of β is used and correct values when the correct version of β is used instead.

The available experimental data of the samples under study are obtained under a similar setup to that of Ref. [8]. Contrary to the previous work [5], the current numerical simulation considers the photoconductivity σ_{ph} as an additional free parameter for the a-Si: H sample (where the experimental value is not available). This parameter is employed alongside the four free parameters of electron mobility (μ_n), hole mobility (μ_p), recombination lifetime (τ), and $\frac{G_1\tau}{N_o}$ (where G_1 is the amplitude of modulated generation rate ΔG [1-9] and N_o is free plus trapped carrier density under uniform illumination). This is done in order to reproduce the experimental field-dependent data of this sample. However, the photoconductivity σ_{ph} is fixed for both nanocrystalline samples and is used as given by the photoconductivity experiment [12]. The ratio $\frac{I_2}{I_1}$ (where I_2 and I_1 are the chopped and main light intensities, respectively) is kept fixed as measured from the experiment [12]. Furthermore, the experimental filed-dependent data of two nc-Si: H samples are also analyzed using L and $\phi(=\gamma\gamma_o^2)$ (where γ is the exponent of the power-law relation between photoconductivity and generation rate due to uniform intensity G_o, while γ_o is a grating factor between zero and unity [12]) as free parameters besides the other above-mentioned four parameters.

2. A Brief Outline of Theoretical Approach

In regard to the SSPG technique, the adopted theoretical approach concerned with solving coupled non-linear differential equations (NLDEs) to get expressions for photocarrier densities of both electrons and holes was presented elsewhere [8]. The latter expressions were employed to find the expression of β (Λ, E_o). Here, β (Λ, E_o) was found to be dependent on both Λ and electric field E_o. Moreover, β (Λ, E_o) was found sensitive to other physical parameters, namely, L, τ, μ_n, and μ_p that shape the photoelectronic behaviors of noncrystalline semiconductors. Regarding the application of the derived expression on different types of semiconductors, the same assumptions used elsewhere will be adopted in this work. Now, β (Λ, E_o) has the following formula [5]:

$$\beta = 1 - \frac{aI_r}{2S'}\left(\frac{G_1\tau}{N_o}\right)^2 (T_a + T_d), \quad (1)$$

where

$$I_r = 1 + \frac{I_1}{\gamma I_2}, \quad (2)$$

$$S' = (a - \frac{(b+1)^2}{2(1+b^2)}), \quad (3)$$

$$T_a = \frac{W_d}{W^2}(T_{a1} + T_{a2} + T_{a3} + T_{a4}), \quad (4)$$

with

$$W_d = (a + \frac{\ell^2}{4b}(1+b)^2)(1+\ell^2) + d^2, \quad (5)$$

and

$$W = W_d^2 + \frac{d^2}{4b}(b-1)^2. \quad (6)$$

Also,

$$T_d = \frac{d^2(b-1)^2}{2W^2(1+b^2)}[d^2 + \frac{(1+b)^2}{4b}\ell^4 + \frac{a(1+b)^2}{2b}\ell^2 + \frac{a(b-1)^2}{4b} + \frac{a^2(1+b^2)}{b}], \quad (7)$$

and

$$T_{a1} = a^2[a + \ell^4(1 + \frac{(1+b)^2}{4b}) + \ell^2(1 + a + \frac{(1+b)^2(b-1)^2}{4b(1+b^2)}) - \frac{2b}{1+b^2}(1 + \frac{(1+b)(b-1)^2}{8b(1+b^2)})], \quad (8)$$

$$T_{a2} = a\frac{(1+b)^2}{(1+b^2)}[\frac{(1+b^2)}{4b}\ell^6 - \frac{\ell^4}{2}(1 + \frac{(1+b)^2}{4b}) - \ell^2(1 + \frac{(b-1)^2}{8b})], \quad (9)$$

$$T_{a3} = d^2[(a + \ell^2)(a - \frac{(1+b)^2}{2(1+b^2)}) - \frac{(b-1)^2}{2(1+b^2)}], \quad (10)$$

$$T_{a4} = -\frac{(1+b)^4}{8b(1+b^2)}\ell^4(1+\ell^2). \quad (11)$$

Here, $a(=\frac{\tau}{\tau_{diel}})$, $b(=\frac{\mu_n}{\mu_p})$, $\ell = \frac{2\pi L}{\Lambda}$, and $d = \frac{2\pi\tau E_o}{\Lambda}\sqrt{\mu_n\mu_p}$, which are as defined elsewhere [1-9], comprise sensitive physical parameters, namely, τ, τ_{diel}, μ_n, μ_p, L, Λ, and E_o, in addition to other sensitive parameters that exist in both β expressions, namely, $\frac{G_1}{N_o}$ and $\frac{I_2}{I_1}$ [1-9]. Here, we assumed that μ_n and μ_p are the average mobilities of all free and trapped electrons and holes, respectively, while τ is the photocarrier common recombination lifetime which is considered in the case of prevalence of ambipolar conditions where trapping times of photocarriers are very small compared to the small signal photocurrent response time [5]. However, the parameter γ, as defined in Ref. [8], represents the exponent in the power law intensity dependence of current density or as defined earlier, the exponent in the power law relation between photoconductivity and generation rate due to uniform intensity G_o [1,8]. Moreover, it must be noted that an assumption is made such that $N_o=P_o$ and $G_o=R_o$ (where P_o and R_o represent free plus trapped hole density and recombination rate under uniform background illumination, respectively) [5]. The free parameters used in the simulation process are μ_n, μ_p, τ, and $\frac{G_1}{N_o}$. It must be recalled that G_1 is the amplitude of the generation rate, while N_o is the trapped and free carrier density under uniform illumination G_o. Also, in some cases, the photoconductivity σ_{ph} or the parameter ϕ can be considered as a free parameter [1]. The relation between G_o and σ_{ph} is given by [5]:

$$G_o = \frac{\sigma_{ph}}{e(\mu\tau)_n}. \quad (12)$$

Here, $(\mu\tau)_n$ is the mobility-lifetime product for electrons. The photoconductivity is defined as:

$$o_{ph} = eN_o(\mu_n + \mu_p). \quad (13)$$

Moreover, the dielectric relaxation time of the semiconductor τ_{diel} has the expression [10]:

$$\tau_{diel.} = \frac{\varepsilon\varepsilon_o}{\sigma_{ph}}, \quad (14)$$

Here, ε_o and ε are the dielectric permittivities of the vacuum and semiconductor material, respectively.

The corrected expression β' constitutes of β, as seen in Eq. (1), and the correction factor $\delta\beta$, namely [5]:

$$\beta' = \beta + \delta\beta. \quad (15)$$

where $\delta\beta$ is written as:

$$\delta\beta = -\frac{aI_r}{2S'W^2}\left(\frac{G_1\tau}{N_o}\right)^2 (\frac{a}{(1+b)(1+b^2)})[\frac{b}{d^2}\{N_1\delta P_2 + P_1\delta N_2 + \delta P_1\delta N_2\} + P_1 + \delta P_1 + N_2\delta P_1]. \quad (16)$$

where N_1, N_2, P_1, δP_1, δP_2, and δN_2 are defined elsewhere [5].

A Fortran program was developed using both expressions β (approximate) and β' (corrected)

and incorporating a subroutine that can evaluate the value of χ^2. Thus, the reproduced field-dependent data are optimized using this value of χ^2 as an indicator.

3. Results and Analysis

Our derived (approximate and corrected) expressions of β can be examined using available field-dependent data collected at room temperature for different grating periods from the SSPG technique for *a*-Si: H sample and two *nc*-Si: H samples prepared by plasma enhanced chemical vapor deposition technique [8, 12]. The calculated values of field-dependent β (approximate and correct) are compared to the corresponding experimental data taken for different grating periods. For *a*-Si: H, the grating periods include 1180, 1880, 2580, and 3290 nm, as shown in Fig. 1. For *nc*-Si: H # I, the grating periods comprise 1180, 2230, and 3290 nm, as presented in Fig. 2. Finally, for *nc*-Si: H # II, the grating period is 2580 nm, depicted in Fig. 3. The best fitting is reached when χ^2 is minimum using the approximate or correct expression of β. The value of L, obtained from low electric field data, is 145 nm for the *a*-Si: H sample and the ratio $\frac{I_2}{I_1}$ is equal to 0.0063. Using the value L = 145 nm, $(\mu\tau)_n \sim 3.1\times 10^{-7}$ cm^{2}V^{-1}, $\phi = 0.34$, as obtained from the fit of low field data [12, 14], and the average approximate and correct values of photoconductivity from our results of simulation $\sigma_{ph} \sim 1.275 \times 10^{-5}$ and $\sim 1.13\times 10^{-5}$ S cm^{-1} [12], one can get $G_o \sim 2.572\times 10^{20}$ and 2.280×10^{20} cm^{-3} for the approximate and correct values, respectively. Thus, using Eq. (13) and obtained fitting parameters (approximate and correct), one can determine the values of N_o (approximate and correct) at different grating periods and the results are listed in Table 1. Moreover, $G_1\tau$ and G_1 can be obtained from our analysis. At grating periods of 1180, 1880, 2580, and 3290 nm, the approximate values of G_1 are 4.70×10^{19}, 8.91×10^{19}, 1.90×10^{19}, and 1.88×10^{19} cm^{-3} s^{-1}, respectively, while the correct corresponding values are 4.49×10^{19}, 18.26×10^{19}, 4.43×10^{19}, and 3.56×10^{19} cm^{-3} s^{-1}. Therefore, the approximate values of ratio $\frac{G_1}{G_o}$ are 0.182, 0.346, 0.074, and 0.073 while the correct corresponding values are 0.197, 0.800, 0.194, and 0.156, for the grating periods of 1180, 1880, 2580 and 3290 nm, respectively. These results indicate that the linearity conditions required for solving the nonlinear differential equations of our method are satisfied.

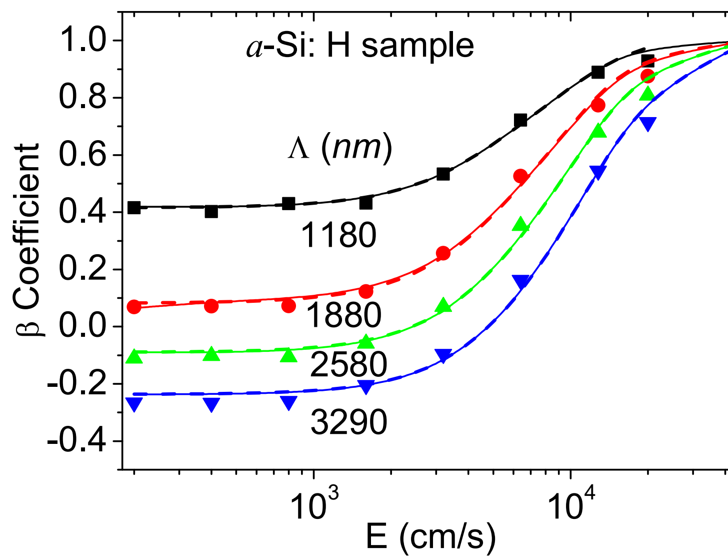

FIG. 1. The variation of β vs. electric field at different grating periods for *a*-Si: H sample at room temperature. The dashed and solid lines represent the theoretical results obtained by applying the approximate and corrected formulas of β, respectively, as compared to the corresponding experimental data (symbols).

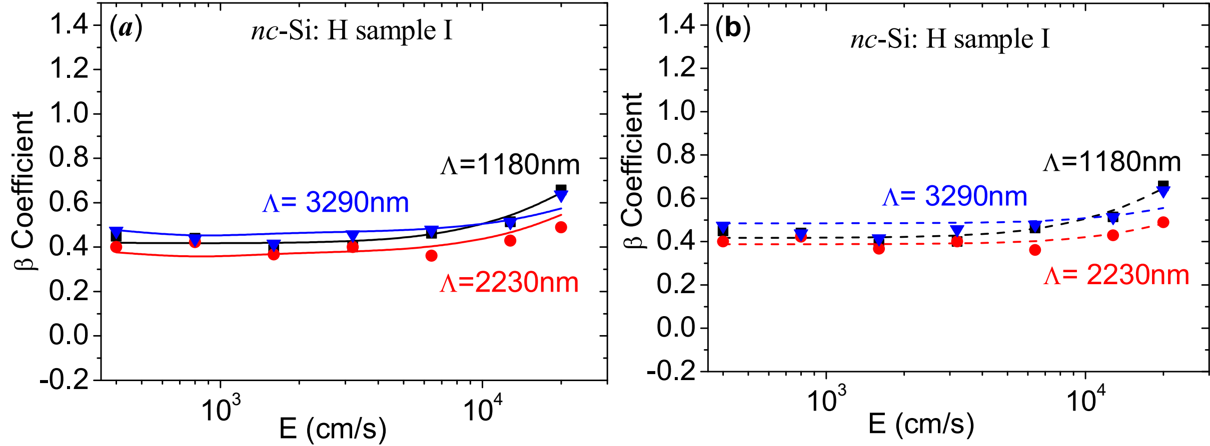

FIG. 2. The plot of β vs. electric field at different grating periods for *nc*-Si: H sample I at room temperature. Theoretical results (a) (solid line) using the correct expression of β (b) (dashed lines) using the approximate expression of *β*, as compared to experimental data (symbols)

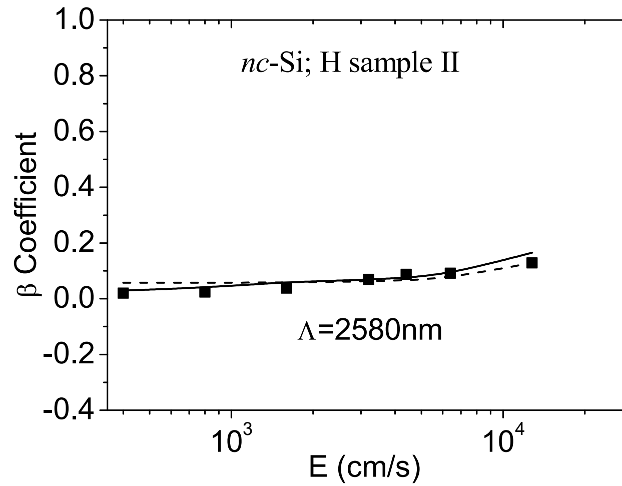

FIG. 3. The plot of β vs. electric field at single grating period for nc-Si: H sample II at room temperature. Theoretical results using correct and approximate expressions of *β,* (solid line) and (dashed line), respectively, as compared to experimental data (symbols).

For *nc*-Si: H samples # I and II, the value of $\frac{I_2}{I_1} = 0.0063$ is also used as a fixed parameter. The best fit to the experimental data (Figs. 1 and 2) is obtained when adjustable parameters μ_n, μ_p, τ, L, ϕ, and $\frac{G_1}{N_o}$ are used and χ^2 is the minimum. All parameters are listed in Table 2. A simple photoconductivity experiment shows that the photoconductivity $\sigma_{ph} \sim 1.97 \times 10^{-5}$ S cm^{-1} and ~ 2.56× 10^{-5} S cm^{-1}, and electron mobility lifetime-product $(\mu\tau)_n \sim 3.37 \times 10^{-7}$ cm^{2}V^{-1} s^{-1} and ~ 3.25× 10^{-7} cm^{2}V^{-1} s^{-1} for *nc*-Si: H samples # I and II, respectively [12]. In a similar analysis as before, we can get $G_o \sim 3.65 \times 10^{20}$ and 4.92×10^{20} cm^{-3} s^{-1}, for samples # I and II, respectively. The determined values of N_o for sample # I, at 1180, 2230, and 3290 nm are listed in Table 2.

The approximate values of G_1 are ~ 8.89×10^{20}, 5.99×10^{20}, and 3.999×10^{20}cm^{-3} s^{-1}, at grating periods of 1180, 2230, and 3290 nm, respectively, for sample I, and ~ 8.178×10^{20} cm^{-3} s^{-1}, at a single grating period of 2580 nm for sample II. However, the correct corresponding values of G_1 are ~ 1.985×10^{20}, *4.971* × 10^{20}, 3.092×10^{20} cm^{-3} s^{-1}, for sample I, and ~ 6.58×10^{20} cm^{-3} s^{-1}, for sample II. The approximate values of G_1 give the values of the ratio $\frac{G_1}{G_o}$ ~ 2.43, 1.64, and 1.095 for sample I and ~ 1.66 for sample II that correspond to the relevant above-mentioned grating periods for each sample. But the correct values of G_1 give the values of the ratio $\frac{G_1}{G_o}$ ~ 0.544, 1.362, and 0.8 for sample I and ~ 1.34 for sample II, with corresponding grating periods. Although the latter corrected values are lesser than the approximate ones, this does not improve much the requirements needed to fulfill the linearity conditions for solving the nonlinear

differential equations when $G_1 > G_o$. Furthermore, both experimental data and theoretical results show that the nc-Si: H sample I has inconsistent behavior at different grating periods. Moreover, the estimated average value of approximate and correct values of ambipolar diffusion length ~ 96.6 and 101.8 nm disagree with the one of 86 nm obtained from low field analysis. Thus, we can conclude that this sample is poorly conductive. However, our method is able to well-reproduce the experimental field-dependent data, and the estimated approximate or correct value of L ~ 55 nm for sample II from this analysis, has better agreement with the estimated one of ~ 54 nm from low field analysis.

Overall, the values of hole mobility obtained from the SSPG analysis at room temperature do not agree with those measured by other techniques, such as the field-effect hole mobility measurement, by two to three orders of magnitude [18].

TABLE 1. The results of photoelectronic parameters from modeling the available field-dependent data for a-Si: H at 300K. These results are obtained when the χ^2 indicator is minimum. Both $(\frac{I_2}{I_1}) = 0.0063$ and L = 145 nm are inserted as fixed entrees during the fitting process.

	a-Si:H at 300K			
Λ (nm)	1180	1880	2580	3290
$\mu_n^c\ (cm^2V^{-1}s^{-1}) \times 10^{-2}$	1.22	1.000	1.007	1.006
$\mu_n^a\ (cm^2V^{-1}s^{-1}) \times 10^{-2}$	1.11	1.099	0.989	1.014
$\mu_p^c\ (cm^2V^{-1}s^{-1}) \times 10^{-3}$	0.798	0.397	0.397	0.399
$\mu_p^a\ (cm^2V^{-1}s^{-1}) \times 10^{-3}$	1.016	0.969	0.697	0.748
$\tau^c\ (s) \times 10^{-5}$	1.570	0.406	1.657	1.945
$\tau^a\ (s) \times 10^{-5}$	1.614	0.808	4.081	3.968
$\sigma^c_{ph}\ (Scm^{-1}) \times 10^{-5}$	2.889	0.243	0.663	0.730
$\sigma^a_{ph}\ (Scm^{-1}) \times 10^{-5}$	3.458	1.008	0.259	0.264
$(\frac{G_1\tau}{N_o})^c$	0.1298	0.1092	0.1102	0.1027
$(\frac{G_1\tau}{N_o})^a$	0.1299	0.1221	0.1167	0.1149
$(\frac{G_1}{N_o})^c\ (s^{-1}) \times 10^4$	0.827	2.690	0.665	0.528
$(\frac{G_1}{N_o})^a\ (s^{-1}) \times 10^4$	0.807	1.511	0.286	0.289
$(N_o)^c\ (cm^{-3}) \times 10^{15}$	5.43	6.79	6.75	6.75
$(N_o)^a\ (cm^{-3}) \times 10^{15}$	5.83	5.9	6.67	6.51
$(\chi^2)^c$	0.495	0.125	2.053	2.570
$(\chi^2)^a$	0.493	0.159	2.135	2.672

^{c} and ^{a} represent the corrected and approximates values, respectively.

TABLE 2. List of parameters used to fit the experimental data of field-dependent β obtained at different values of the grating period for two different *nc*-Si: H samples at room temperature. The ratio $(\frac{I_2}{I_1})$ = 0.0063.

	nc-Si:H sample I at 300K			*nc*-Si:H sample II at 300K
Λ (nm)	1180	2230	3290	2580
$\mu_n^c\,(cm^2V^1s^{-1}) \times 10^{-2}$	0.588	1.460	1.860	1.907
$\mu_n^a\,(cm^2V^1s^{-1}) \times 10^{-2}$	1.219	1.133	1.860	1.907
$\mu_p^c\,(cm^2V^1s^{-1}) \times 10^{-3}$	0.147	0.700	0.700	0.694
$\mu_p^a\,(cm^2V^1s^{-1}) \times 10^{-3}$	0.719	0.639	0.700	0.694
$\tau^c\,(s) \times 10^{-6}$	6.889	0.788	0.788	0.770
$\tau^a\,(s) \times 10^{-6}$	0.713	0.798	0.788	0.770
ϕ^c	0.48	0.5	0.5	0.46
ϕ^a	0.48	0.5	0.5	0.46
L^c(nm)	106.8	99.3	99.3	45.00
L^a(nm)	91.37	99.1	99.3	45.00
$(\frac{G_1\tau}{N_o})^c$	0.0661	0.0468	0.0382	0.0609
$(\frac{G_1\tau}{N_o})^a$	0.0665	0.0465	0.0494	0.0779
$(\frac{G_1}{N_o})^c\,(s^{-1}) \times 10^4$	0.959	5.940	4.847	7.909
$(\frac{G_1}{N_o})^a\,(s^{-1}) \times 10^4$	9.326	5.827	6.269	10.116
$(N_o)^c\,(cm^{-3}) \times 10^{15}$	20.7	8.370	6.38	8.32
$(N_o)^a\,(cm^{-3}) \times 10^{15}$	9.54	10.28	6.38	8.085
$(\chi^2)^c$	0.498	3.723	2.233	0.622
$(\chi^2)^a$	0.526	0.477	2.154	0.503

^{c} and ^{a} represent the corrected and approximates values, respectively.

4. Conclusion

The success of our method in analyzing the experimental field-dependent data for the chosen samples asserts the validity of this method and encourages its use for different categories of noncrystalline samples. Our approach shows the transparent relationship between the transport parameters and the trapped charge carrier density. In particular, it can provide a basis for understanding the enhanced relationship between the product of minority carrier mobility and lifetime and the trapped charge density, as well as the sub-gap absorption observed in the three samples under investigation. Although this reflects the fact that the parameters of charge carrier mobility depend on carrier charge concentration, it presents a weakness in the assumptions regarding local charge neutrality and ambipolar restriction. The advantages of our approach enable us to determine approximate and corrected values for each extracted parameter. This allows us to estimate the degree of accuracy in each parameter and may lead to a better estimation of charge carrier density in addition to the ambipolar diffusion length for the good conductive samples with the exclusion of the poorly conductive sample.

Acknowledgments

The authors are grateful to Dr Rudi Brueggemann at Oldenburg University, Germany, and to H. Brummack and K. Bruhne, Institute fur Physikalische Elektronik, Universitat Stuttgart, for providing the experimental data and samples.

References

[1] Ritter, D., Zeldov, E. and Weiser, K., Appl. Phys. Lett., 49 (13) (1986) 791.

[2] Ritter, D., Weiser, K. and Zeldov, E., J. Appl. Phys., 62 (11) (1987) 4563.

[3] Ritter, D., Weiser, K. and Zeldov, E., Phys. Rev. B, 38 (12) (1988) 8296.

[4] Li, Y.-M., Phys. Rev., 42 (14) (1990) 9025.

[5] Badran, R.I., Results Phys., 17 (2020) 103079.

[6] Hattori, K., Okamoto, H. and Hamakawa, Y., Phys. Rev. B, 45 (3) (1992) 1126.

[7] Balberg, I., Phys. Rev. B, 44 (4) (1991) 1628.

[8] Badran, R.I., J. Mater. Sci. Mater. Electron., 18 (4) (2007) 405.

[9] Abel, C.D., Bauer, G.H.. and Bloss, W.H., Philos. Mag. B Phys. Condens. Matter; Stat. Mech. Electron. Opt. Magn. Prop., 72 (5) (1995) 551.

[10] Brüggemann, R., J. Phys. Conf. Ser., 253 (1) (2010) 012081.

[11] Sauvain, E. and Chen, J.H., J. Appl. Phys., 75 (10) (1994) 5191.

[12] Badran, R.I. and Al-Awwad, N., J. Optoelectron. Adv. Mater., 8 (4) (2006) 1466; Al Awaad, N., MSc Thesis, The Hashemite University, (2005).

[13] Badran, R.I., J. Optoelectron. Adv. Mater., 10 (1) (2008) 174.

[14] Badran, R.I., Brüggemann, R. and Carius, R., J. Optoelectron. Adv. Mater., 11 (10) (2009) 1464.

[15] Yadav, D. and Agarwal, S.C., Solid State Commun., 150 (7–8) (2010) 321.

[16] Niehus, M. and Schwarz, R., Phys. Status Solidi Curr. Top. Solid State Phys., 3 (6) (2006) 2103.

[17] Zweigart, S., Menner, R., Klenk, R. and Schock, H.W., Mater. Sci. Forum, 173–174 (1995) 337.

[18] Cheng, I.C. and Wagner, S., Appl. Phys. Lett., 80 (3) (2002) 440.